

Multi-stability and FPGA Implementation of a Conservative Chaotic System

Minghan Song

College of Electronic Information and Automation, Tianjin University of Science and Technology,
300222, China;

E-mail: *892095883@qq.com

www.tust.edu.cn

Abstract

The paper first studies the reason why a three-dimensional volume conservative chaotic system proposed by Vaidyanathan and Volos can generate chaos by analyzing mechanics and energy. Then, based on numerical methods including balance characteristics, Lyapunov exponents, bifurcation diagrams, phase trajectories and so on, multi-stability of the three-dimensional volume conservative chaotic system are discovered. In addition, the three-dimensional volume conservative chaotic system is realized by using FPGA, and all the results from FPGA implementation are consistent with those from numerical analysis.

Keywords: Chaos, Conservative, Multi-stability, FPGA implementation

1. Introduction

In 1964, Hénon and Heiles proposed a conservative chaotic system for the first time in the study of three-body motion, which was called the Hénon-Heiles system^{1,2}. In 1994, Sprott proposed some simple three-dimensional chaotic systems, it is often called Sprott-A system³. This system is actually a special case of the Nosé-Hoover system, also known as the Nose-Hoover conservative oscillator⁴⁻⁶. Subsequently, in 1997 and 1999, Sprott and Thomas respectively gave the jerk conservative chaotic system and the conservative chaotic system with sine function⁷⁻⁸. Subsequent research on conservative chaotic characteristics is gradually attracting researchers' attention⁹⁻¹⁵.

In addition, in recent years, chaotic systems with multi-stability characteristics are gradually becoming a hot issue in chaotic theory and application research¹⁶⁻²¹. Multi-stability phenomenon usually refers to the phenomenon that different manifolds coexist in the system when different initial values are taken when the system parameters are unchanged. In particular, when the

initial value of the system is changed, the number of manifolds tends to be infinite, this phenomenon is called super multi-stability²²⁻²⁴. Multi-stability is ubiquitous in many natural systems and usually has an important impact on system performance. Although there are no attractors in conservative systems, they are extremely sensitive to small fluctuations under initial conditions. Due to the existence of multiple stability, the system is extremely sensitive to small disturbances under initial conditions, which often leads to the coexistence of multiple streams. This uncertainty and complexity also attract more and more attention^{25,26}.

The rest of the paper is organized as follows: in Section 2, we conduct a mechanical analysis of a three-dimensional conservative chaotic system and reveal the cause of chaos. Then We conduct research on whether the system produces multi-stability in Section 3. After that, FPGA implementation of this system is showed in Section 4, while Section 5 concludes the paper.

2. A three-dimensional conservative chaotic system and its analysis

In 2013, Vaidyanathan and Volos⁹ proposed a three-dimensional volumetric conservative chaotic system, which was described as:

$$\begin{cases} \dot{x} = xz + ay \\ \dot{y} = yz - bx \\ \dot{z} = 1 - x^2 - y^2 \end{cases} \quad (1)$$

Among them, x, y, z are state variables, a and b are state parameters. When setting $a=0.05, b=1$, the calculated Lyapunov exponent is:

$$L_1 = 0.0395, L_2 = 0, L_3 = -0.0395 \quad (2)$$

It can be seen that the sum of Lyapunov exponents of system (1) is 0, so the system is a conservative chaotic system.

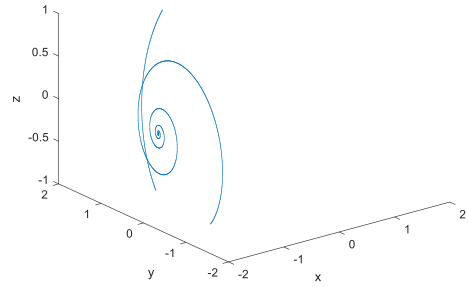
When choosing different initial values and parameters of the system, the system can also present rich periodic or chaotic dynamics. In order to further study the reasons for the chaotic dynamics of the system (1) from the perspective of energy characteristics, first convert it into the Kolmogorov form as:

$$\dot{x} = J(x)\nabla H(x) + u = \begin{bmatrix} 0 & a & x \\ -b & 0 & y \\ -x & -y & 0 \end{bmatrix} \begin{bmatrix} x \\ y \\ z \end{bmatrix} + \begin{bmatrix} 0 \\ 0 \\ 1 \end{bmatrix} \quad (3)$$

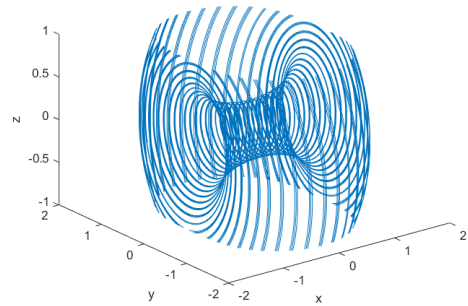
where, $J(x) = \begin{bmatrix} 0 & a & x \\ -b & 0 & y \\ -x & -y & 0 \end{bmatrix}$, $u = \begin{bmatrix} 0 \\ 0 \\ 1 \end{bmatrix}$,

$H(x) = \frac{1}{2}(x^2 + y^2 + z^2)$. Through the analysis, it can be found that the system (3) consists of two parts: the conservative moment $J(x)\nabla H(x)$ and the external moment u .

When we set $a=b=10$, take the initial value $(x, y, z) = (1, 1, 1)$, the phase diagram under the action of conservative moment and the phase diagram under the action of conservative moment and external moment are obtained, as shown in Fig. 1. From Fig.1, it can be seen that the external torque is the main reason for the chaotic phenomenon of the system.



(a) Phase diagram under conservative torque



(b) Phase diagram under the combined action of conservative torque and external torque

Fig.1 Phase diagram

3. Multi-stability analysis of the three-dimensional conservative chaotic system

Generally, systems with hidden attractors are extremely sensitive to initial values, and there will often be situations where multiple attractors coexist, that is called multi-stability. Multi-stability means that when the system parameters are fixed, corresponding to different initial values, the system presents different dynamic characteristics, and the corresponding phase diagram will also show different attractors.

3.1. $a \neq b$

When we select the initial value of the system (1) $(x, y, z) = (1, y_0, -3)$, the parameters $a=1, b=1.6$, where y_0 varies from -5 to 5 , and the Lyapunov exponent diagram and bifurcation diagram that vary with y_0 are shown in Fig.2 and Fig.3. It can be seen that when $y_0 \in (-5, -4.3) \cup (-3.3, 0.2) \cup (1.5, 5)$, the maximum Lyapunov exponent of the system is greater than 0, and the system is in a chaotic state; when $y_0 \in (-4.3, -3.3) \cup (0.2, 1.5)$,

the motion state of the system changes between cycles and counter cycles. When we select the initial value $(x, y, z) = (1, -2.75, -3)$, the phase diagram and Poincaré cross-sectional diagram drawn are shown in Fig.4 and Fig.5. It can be seen that the system (1) is in a state of chaos.

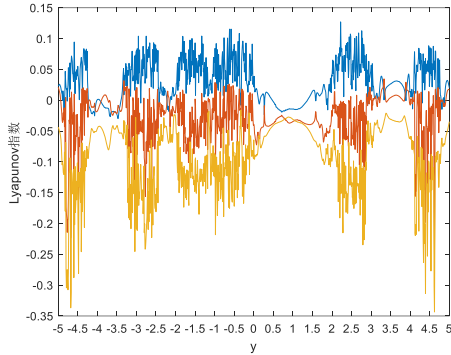


Fig.2 Lyapunov exponent diagram with yo

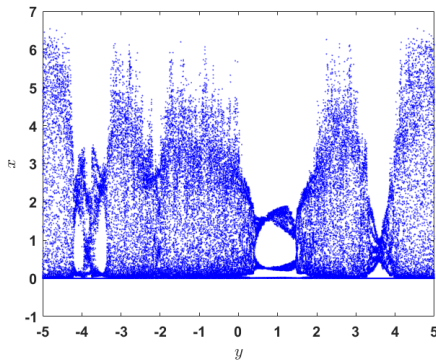


Fig.3 Bifurcation diagram

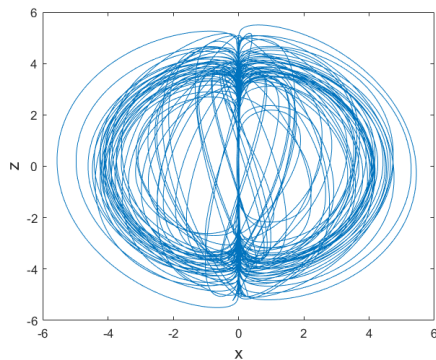


Fig.4 Phase diagram

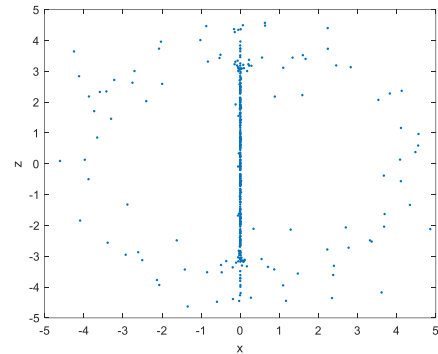


Fig.5 Poincaré cross-sectional diagram

We further analyze system (1), when selecting different initial values, we find hidden attractors in the system. For example, when we select the initial value $(x, y, z) = (1, -4, -3)$, $(1, 1, -3)$, $(1, 3.75, -3)$, the system will have three quasi-periodic attractors in different states as shown in Fig.6, which are represented by red, blue and green lines respectively. When we select $(x, y, z) = (1, -4.5, -3)$, $(1, -1, -3)$, the system will show two quasi-periodic attractors in different states as shown in Fig.7, which are represented by blue and red lines respectively. When we select $(x, y, z) = (1, 0.76, -3)$, $(1, 3.64, -3)$ is selected, the system will show two different states of periodic attractors as shown in the figure, which are represented by blue and red lines respectively. The above numerical analysis fully shows that when $a \neq b$, system (1) has multi-stability.

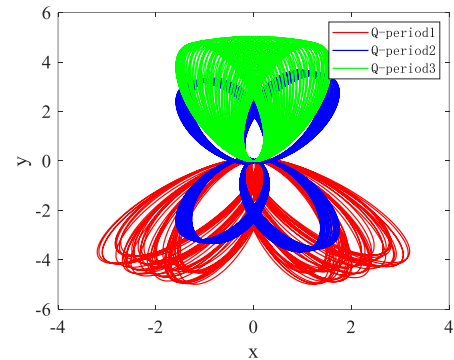


Fig.6 Three quasi-periodic attractors

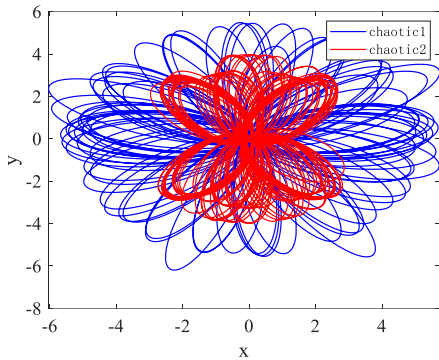


Fig.7 Two chaotic attractors

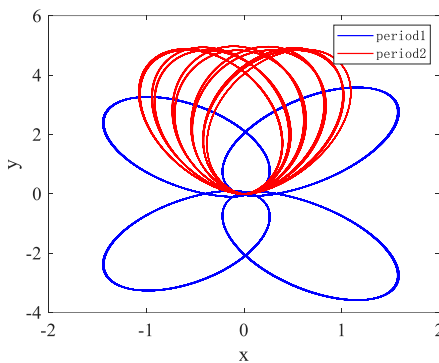


Fig.8 Two period attractors

3.2 a=b

When we select the initial value of the system (1) $(x, y, z) = (x_0, 1, 1)$, the parameters $a=b=1$, where x_0 varies from -5 to 5, and the Lyapunov exponent diagram and bifurcation diagram that vary with x_0 are shown in Fig.9 and Fig.10. It can be seen that when $x_0 \in (-5, -0.5) \cup (0.5, 5)$, the maximum Lyapunov exponent of the system is greater than 0, and the system is in a chaotic state; when $x_0 \in (-0.5, 0.5)$, the motion state of the system changes between cycles and counter cycles.

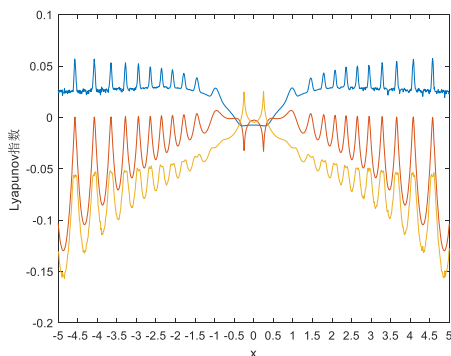


Fig.9 Lyapunov exponent diagram with x_0

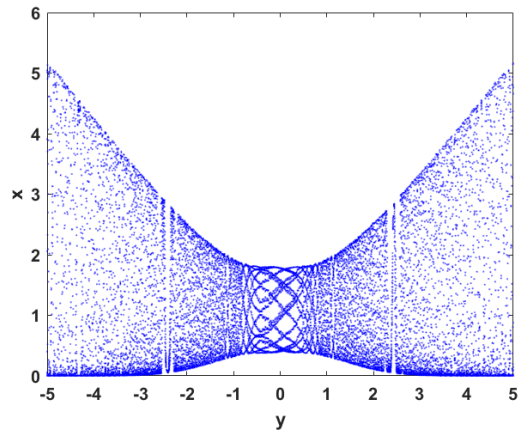
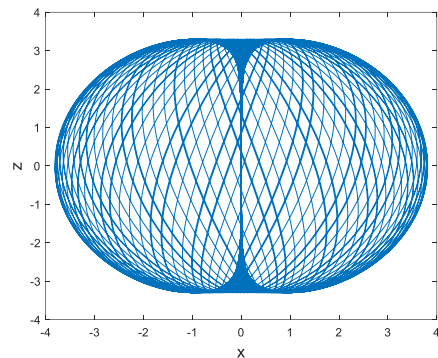
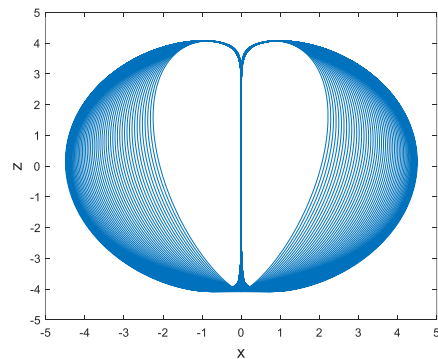


Fig.10 Bifurcation diagram

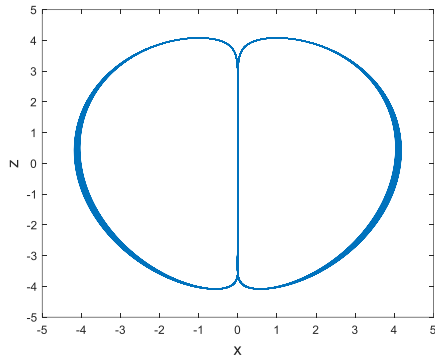
Then we further study the multi-stability of system (1) in this state. Select the initial value $(x, y, z) = (2, -1.45, -2.75)$, $(2, -1.85, -3.5)$, $(2, -3.8, 1.45)$, respectively, and system (1) will appear chaotic, quasi-periodic, and periodic attractors, as shown in Fig.11. Through the above numerical analysis, when $a=b$, system (1) exhibits multiple stability phenomena.



(a) Phase diagram with $(x, y, z) = (2, -1.45, -2.75)$



(b) Phase diagram with $(x, y, z) = (2, -1.85, -3.5)$



(c) Phase diagram with $(x, y, z) = (2, -3.8, 1.45)$

Fig.11 System phase diagram under different initial values

4. FPGA implementation of the three-dimensional conservative chaotic system

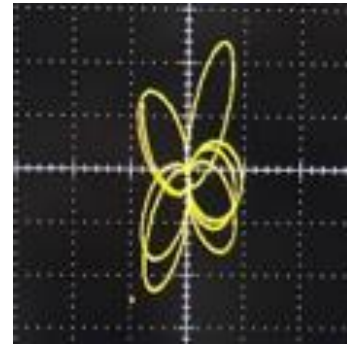
The FPGA hardware device used in this article is the DE2i-150 development board. First, we model and design system (1) and build its circuit structure model. Then the circuit model is converted into the corresponding FPGA hardware description language VHDL through Signal Compiler, for synthesis, compilation, adaptation and simulation. Finally, download the generated file to the FPGA hardware development board, and observe the image by debugging the oscilloscope.

When designing the circuit model, since system (1) is a continuous-time chaotic system, it needs to be discretized and converted into a digital circuit, which is built through the MATLAB/Simulink library. The equation discretized by Euler algorithm is:

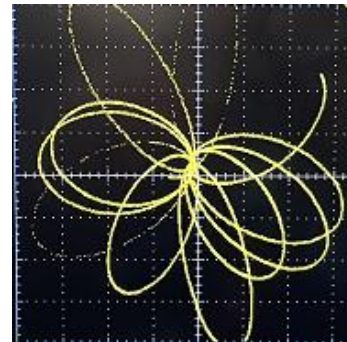
$$\begin{cases} x(n+1) = x(n) + \Delta T[x(n)z(n) + ay(n)] \\ y(n+1) = y(n) + \Delta T[y(n)z(n) - bx(n)] \\ z(n+1) = z(n) + \Delta T[1 - x(n)x(n) - y(n)y(n)] \end{cases} \quad (4)$$

among them, ΔT is the sampling time; $x(n)$, $y(n)$, $z(n)$ are the iterative sequence in the current state; $x(n+1)$, $y(n+1)$, $z(n+1)$ are the iterative sequence in the next cycle state.

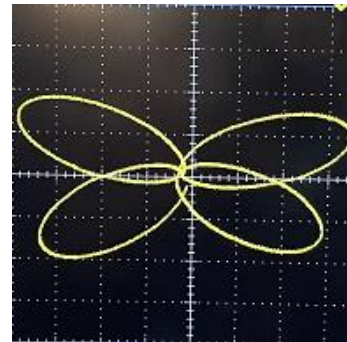
Take the parameters $a=1$, $b=1.6$, the initial value $(x, y, z) = (1, 1, -3)$, $(1, -1, -3)$, $(1, 0.76, -3)$, and the phase diagram observed by the oscilloscope is shown in the Fig.12(a)-(c). It can be found from Fig.12 that the FPGA hardware implementation results are consistent with the numerical analysis results, which further verifies the physical feasibility and multi-stability of system (1).



(a) Phase diagram with $(x, y, z) = (1, 1, -3)$



(b) Phase diagram with $(x, y, z) = (1, -1, -3)$



(c) Phase diagram with $(x, y, z) = (1, 0.76, -3)$

Fig.12 When taking different initial values and parameters, the system phase diagram observed by the oscilloscope

5. Conclusion

By analyzing the mechanical properties of the three-dimensional conservative chaotic system proposed by Vaidyanathan and Volos, the reasons for the chaos of the system are revealed. Then by changing the system parameters and initial values, it is found that the system has rich dynamic behaviors, including periodic characteristics, quasi-periodic characteristics, and chaotic characteristics. In addition, the rich dynamic characteristics of the three-dimensional system are

verified from the perspectives of numerical analysis and FPGA implementation, and the FPGA hardware experimental results are consistent with the numerical analysis results, which further demonstrates the physical feasibility of the system in a physical sense.

References

1. Hénon M, Helles C. The applicability of the third integral of motion: Some numerical experiments. *Astrophys J*, 1964, 69: 73-79
2. Lakshmanan M, Rajasekar S. Nonlinear Dynamics - Integrability, Chaos, and Patterns. *Springer-Verlag Berlin Heidelberg*, 2003.
3. Sprott J C. Some simple chaotic flows. *Phys Rev E*, 1994, 50(2): 647-650.
4. Hoover W G. Remark on "some simple chaotic flows". *Phys Rev E*, 1995, 51(1):759-760.
5. Posch H A, Hoover W G, Vesely F J. Canonical dynamics of the Nosé-oscillator: stability, order, and chaos. *Phys Rev A*, 1986, 33: 4253-4265.
6. Hoover W G. Canonical dynamics: equilibrium phase-space distributions. *Phys Rev A*, 1985, 31(3):1695-1697.
7. Sprott J C. Some simple chaotic jerk functions. *Am J Phys*, 1997, 65: 537-543.
8. Thomas R. Deterministic chaos seen in terms of feedback circuits: Analysis, synthesis, labyrinth chaos'. *Int J Bifurcat Chaos*, 1999, 9: 1889-1905.
9. Vaidyanathan S, Volos C. Analysis and adaptive control of a novel 3-D conservative no-equilibrium chaotic system. *Arch Control Sci*, 2015, 25(3): 333-353.
10. Mahmoud G M, Ahmed M E. Analysis of Chaotic and hyperchaotic conservative complex nonlinear systems. *Miskolc Math. Notes*, 2017, 18: 315-326.
11. Singh J P, Roy B K. Five new 4-D autonomous conservative chaotic systems with various type of non-hyperbolic and lines of equilibria. *Chaos Soliton Fract*, 2018, 114: 81-91.
12. Vaidyanathan S, Pakiriswamy S. A 3-D Novel Conservative Chaotic System and its Generalized Projective Synchronization via Adaptive Control. *J Eng Sci Technol Rev*, 2015, 8(2):52-60.
13. Cang shijian, Wu A G, Wang Z H, et al. On a 3-D generalized Hamiltonian model with conservative and dissipative chaotic flows. *Chaos Soliton Fract*, 2017, 99: 45-51.
14. Gugapriya G, Rajagopal K, Karthikeyan A, et al. A family of conservative chaotic systems with cyclic symmetry. *Pramana*, 2019, 92(4):48.
15. Cang shijian, Li Y, Xue Wei, et al. Conservative chaos and invariant tori in the modified Sprott A system. *Nonlinear Dyn*, 2020, 99(2): 1699-1708.
16. Xian Y J, Xia C, Guo T T, et al. Dynamical analysis and FPGA implementation of a large range chaotic system with coexisting attractors. *Results Phys*, 2018, 11: 368-376.
17. Li C B, Sprott J C. Multistability in the Lorenz System: A Broken Butterfly. *Int J Bifurcat Chaos*, 2014, 24: 1450131, 7pages.
18. Bao B C, Hu A H, Bao H, et al. Three-Dimensional Memristive Hindmarsh-Rose Neuron Model with Hidden Coexisting Asymmetric Behaviors. *Complexity*, 2018, Article ID 3872573, 11 pages.
19. Jia Hongyan, Shi W X, Qi G Y. Coexisting attractors, Energy Analysis and Boundary of Lü System, *Int J Bifurcat Chaos*, 2020, 30(3): 2050048, 12 pages.
20. Wang F P and Wang F Q. Multistability and coexisting transient chaos in a simple memcapacitive system. *Chin. Phys. B*, 2020; 29(5): 058502.
21. Zhang S, Zeng Y H, Li Z J, et al. Generating one to four-wing hidden attractors in a novel 4D no-equilibrium chaotic system with extreme multistability. *Chaos*, 2018, 28: 013113, 11 pages.
22. Bao B, Bao H, Wang N, Chen M, Xu Q. Hidden extreme multistability in memristive hyperchaotic system. *Chaos Soliton Fract* 2017;94:102-111.
23. Chen M, Sun M, Bao B, Wu H, Xu Q, Wang J. Controlling extreme multistability of memristor emulator-based dynamical circuit in flux-charge domain. *Nonlinear Dyn* 2018;91(2):1395-1412.
24. Bao H, Jiang T, Chu K, Chen M, Xu Q, Bao B. Memristor-based canonical Chua's circuit: extreme multistability in voltage-current domain and its controllability in flux-charge domain. *Complexity* 2018; 2018(5935637):1-13.
25. Jafari, S., Sprott, J.C., Dehghan, S.: Categories of conservative flows. *Int. J. Bifurc. Chaos* 29(02), 1950021 (2019).
26. Singh, J.P., Roy, B.K.: Five new 4-D autonomous conservative chaotic systems with various type of non-hyperbolic and lines of equilibria. *Chaos Solitons Fractals* 114, 81-91(2018).

Authors Introduction

Mr. Minghan Song



He received his bachelor's degree in building Electrical and Intelligent engineering from Shandong Jianzhu University, China in 2020. He is studying for a master's degree at Tianjin University of Science and Technology, China.
